

# Temperature-Dependent Helix–Coil Transition of an Alanine Based Peptide

Cheng-Yen Huang,<sup>†</sup> Jason W. Klemke,<sup>†</sup> Zelleka Getahun,<sup>‡</sup> William F. DeGrado,<sup>‡</sup> and Feng Gai<sup>\*,†</sup>

Contribution from the Department of Chemistry and Department of Biochemistry & Biophysics, University of Pennsylvania, Philadelphia, Pennsylvania 19104

Received March 26, 2001

**Abstract:** The helix–coil transition of a synthetic  $\alpha$ -helical peptide (the D-Arg peptide), Ac-YGG(KAAAA)<sub>3</sub>-CO-D-Arg-CONH<sub>2</sub>, was studied by static far-UV circular dichroism (CD) and time-resolved infrared spectroscopy coupled with the laser-induced temperature-jump technique for rapid relaxation initiation. Equilibrium thermal unfolding measurements of the D-Arg peptide monitored by CD spectroscopy reveal an apparent two-state helix–coil transition, with a thermal melting temperature around 10 °C. Time-resolved infrared (IR) measurements following a laser-induced temperature jump, however, reveal biphasic (or multiphasic) relaxation kinetics. The fast phase rises within the 20 ns response time of the detection system. The slow phase has a decay lifetime of  $\sim$ 140 ns at 300 K and exhibits monotonic temperature dependence with an apparent activation energy around 15.5 kcal/mol.

## Introduction

The  $\alpha$ -helix is a common structural motif in proteins. Understanding its folding mechanism is therefore important for understanding how large proteins fold. The helix–coil transition has been studied extensively in the past,<sup>1</sup> including recent theoretical<sup>2</sup> and experimental<sup>3</sup> efforts, as well as studies involving the laser-induced temperature-jump (*T*-jump) method.<sup>4–7</sup> Although a detailed mechanism of the helix–coil transition has begun to emerge, controversy still exists. Williams et al.<sup>4</sup> measured a relaxation time of 160 ns for an Ala-based peptide (the Fs peptide that has a sequence of (A)<sub>5</sub>-(AAARA)<sub>3</sub>-ANH<sub>2</sub>) following a *T*-jump from 9.3 to 27.4 °C, by monitoring the amide I' IR absorbance of the peptide backbone. Using a fluorescent probe (MABA) attached at the N-terminus of the

Fs peptide, however, Thompson et al.<sup>5</sup> observed a much faster relaxation process, with a maximum relaxation time of  $\sim$ 20 ns near the midpoint of the thermal melting transition ( $\sim$ 303 K). They attributed this faster relaxation to rapid unzipping/zippering of the helix ends in response to the *T*-jump. Using a “kinetic zipper” model, they have also calculated the decay of the average helix content and their results indicate that a slower rate should account for the transition between the helix-containing and nonhelix-containing structural ensembles, due to the energy barrier associated with the nucleation process. Their simulations also show that both the fast and slow rates depend only weakly on temperature and exhibit a minimum around the thermal melting midpoint. Recently, the same authors<sup>6</sup> reported the observation of a slower relaxation process (220 ns at 300 K) in a 21-residue helical peptide, Ac-WAAAAH<sup>+</sup>-(AAAR<sup>+</sup>A)<sub>3</sub>A-NH<sub>2</sub>, with a tryptophan residue in position 1 to serve as the fluorescent probe. This relaxation is temperature dependent and has an apparent activation energy of  $\sim$ 8 kcal/mol. Using UV resonance Raman as a probe, Lednev et al.<sup>7</sup> also observed a single exponential relaxation process that is weakly temperature dependent for the Fs peptide, following a laser-induced 3-ns *T*-jump. Unexpectedly, they found that the coil to helix transition has a negative activation energy,  $E_a = -1$  kcal/mol, by decomposing the observed relaxation rates into refolding and unfolding rates using a two-state model.<sup>8,23</sup>

<sup>†</sup> Department of Chemistry.

<sup>‡</sup> Department of Biochemistry & Biophysics.

(1) Schellman, J. A. *J. Phys. Chem.* **1958**, *62*, 1485–1494. Zimm, B. H.; Bragg, J. K. *J. Chem. Phys.* **1959**, *31*, 526–535. Lifson, S.; Roig, A. *J. Chem. Phys.* **1961**, *34*, 1963–1974. Poland, D.; Scheraga, H. A. *J. Chem. Phys.* **1966**, *45*, 2071–2090.

(2) Brooks, C. L. *J. Phys. Chem.* **1996**, *100*, 2546–2549. Poland, D. *J. Chem. Phys.* **1996**, *105*, 1242–1269. Duan, Y.; Kollman, P. A. *Science* **1998**, *282*, 740–744. Jun, B.; Weaver, D. L. *J. Chem. Phys.* **2000**, *112*, 4394–4398. Ferrara, P.; Apostolakis, J.; Caflisch, A. *J. Phys. Chem. B* **2000**, *104*, 5000–5010. Hummer, G.; Garcia, A. E.; Garde, S. *Proteins: Struct., Funct., Genet.* **2001**, *42*, 77–84.

(3) Graff, D. K.; Pastrana-Rois, B.; Venyaminov, S. Y.; Prendergast, F. G. *J. Am. Chem. Soc.* **1997**, *119*, 11282–11294. Rohl, C. A.; Baldwin, R. L. *Methods Enzymol.* **1998**, *295*, 1–26. Kallenbach, N. R.; Spek, E. J. *Methods Enzymol.* **1998**, *295*, 26–41. Anderson, N. H.; Dyer, R. B.; Fesinmeyer, R. M.; Gai, F.; Lui, Z.; Neidigh, J. W.; Tong, H. *J. Am. Chem. Soc.* **1999**, *121*, 9879–9880.

(4) Williams, S.; Causgrove, T. P.; Gilmanishin, R.; Fang, K. S.; Callender, R. H.; Woodruff, W. H.; Dyer, R. B. *Biochemistry* **1996**, *35*, 691–697.

(5) Thompson, P. A.; Eaton, W. A.; Hofrichter, J. *Biochemistry* **1997**, *36*, 9200–9210.

(6) Thompson, P. A.; Munoz, V.; Jas, G. S.; Henry, E. R.; Eaton, W. A.; Hofrichter, J. *J. Phys. Chem. B* **2000**, *104*, 378–389.

(7) Lednev, I. K.; Karnoup, A. S.; Sparrow, M. C.; Asher, S. A. *J. Am. Chem. Soc.* **1999**, *121*, 4076–4077. Lednev, I. K.; Karnoup, A. S.; Sparrow, M. C.; Asher, S. A. *J. Am. Chem. Soc.* **1999**, *121*, 8074–8086.

(8) Nishii, I.; Kataoka, M.; Tokunaga, F.; Goto, Y. *Biochemistry* **1994**, *33*, 4903–4909.

(9) Choma, C. T.; Lear, J. D.; Nelson, M. J.; Dutton, P. L.; Robertson, D. E.; DeGrado, W. F. *J. Am. Chem. Soc.* **1994**, *116*, 856–865.

(10) Albericio, F.; Barany, G. *Int. J. Pept. Protein Res.* **1987**, *30*, 206–216.

(11) Turner, D. H.; Flynn, G. W.; Sutin, N.; Beitz, J. V. *J. Am. Chem. Soc.* **1972**, *94*, 1554–1559. Woodruff, W. H.; Dyer, R. B.; Callender, R. H.; Paige, K.; Causgrove, T. P. *Biophys. J.* **1994**, *66*, A397. Ballew, R. M.; Sabelko, J.; Reiner, C.; Gruebele, M. *Rev. Sci. Instrum.* **1996**, *67*, 3694–3699. Yamamoto, K.; Mizutani, Y.; Kitagawa, T. *Biophys. J.* **2000**, *79*, 485–495.

(12) The *T*-jump amplitude was calculated based on the temperature dependence of D<sub>2</sub>O absorbance, similar to that used by Williams et al. (ref 4).

In this work we report the study of the helix–coil transition in a synthetic 19-residue Ala-based helical peptide using laser-induced *T*-jump and time-resolved infrared spectroscopy. We found that the relaxation kinetics of the peptide following a *T*-jump can be described by a biexponential function, as suggested by the “kinetic zipper” model,<sup>5</sup> and the two relaxation rates are well separated in time at 20 °C. Surprisingly, the slow relaxation process has a large yet simple Arrhenius temperature dependence, contradicting some previous results and a theoretical model.<sup>5,7</sup>

## Experimental Section

**Materials.** A standard Fmoc-protocol<sup>9</sup> employing Pal resin<sup>10</sup> was used for peptide synthesis. All samples were purified to homogeneity and characterized by electrospray-ionization mass spectroscopy. For samples used in the infrared experiments, the residual trifluoroacetic acid (TFA) from peptide synthesis, which absorbs at 1672 cm<sup>-1</sup> in the IR and overlaps with the peptide amide I' band, was removed by lyophilization against DCl. For both equilibrium and time-resolved IR experiments, the peptide was dissolved directly in D<sub>2</sub>O and the final concentration was 2–4 mg/mL.

**Equilibrium Infrared and CD Measurements.** CD data were collected on an AVIV 62DS spectropolarimeter using a 1 mm quartz cell. The peptide concentration used in the CD measurements was 290 μM, determined by the optical density of tyrosine at 276 nm using  $\epsilon_{276} = 1450 \text{ cm}^{-1} \text{ M}^{-1}$ . Mean residue ellipticity was calculated using the equation  $\theta_{222} = (\theta_{\text{obs}}/10lc)/r$ , where  $\theta_{\text{obs}}$  is the ellipticity measured at 222 nm in millidegrees,  $l$  is the optical path length (cm),  $c$  is the concentration of the peptide (M), and  $r$  is the number of residues. FTIR spectra were collected on a Nicolet Magna-IR 860 spectrometer using 1 cm<sup>-1</sup> resolution. A split sample cell with 52 μm Teflon spacer and Ca<sub>2</sub>F windows was employed to allow the separate measurements of the sample and reference (D<sub>2</sub>O) under identical conditions. Temperature regulation was controlled by a water bath (Haake K30) with ±0.2 °C precision. In addition, to correct for slow instrument drift, a computer-controlled translation stage was used to move both the sample and reference side in and out of the IR beam alternately, and each time a spectrum corresponding to an average of 8 scans was collected. The final result was usually an average of 32 such spectra, both for the sample and the reference.

**Time-Resolved *T*-Jump Infrared Measurements.** The laser-induced *T*-jump<sup>11</sup> infrared setup used in this study is similar to that reported by Williams et al.<sup>4</sup> Briefly, the 3 ns, 10 mJ, 1.9 μm, and 10

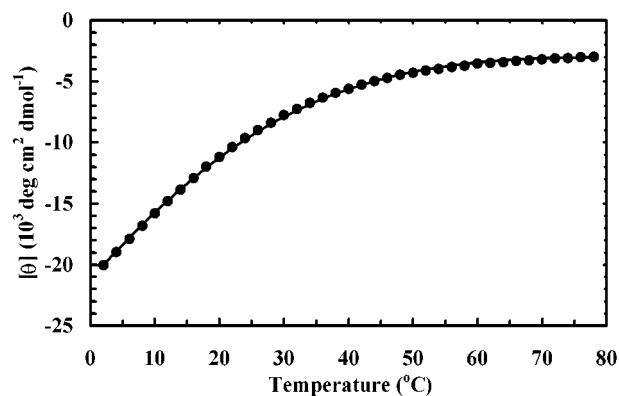


**Figure 1.** Mean residue ellipticities (filled circles) of the D-Arg peptide at 222 nm as a function of temperature. Fitting these data to an apparent two-state model (solid line) yields a thermal melting temperature of 10 °C. The fraction of the helical peptide at each temperature was calculated according to Luo and Baldwin<sup>15</sup> equations with  $N_R = 15$ .

Hz *T*-jump pulse was generated via Raman shifting the Nd:YAG fundamental, 1064 nm (Coherent Infinity 15-30), in H<sub>2</sub> gas pressurized at 750 psi. A *T*-jump of 10–15 °C can be obtained routinely in an approximately 80 nL laser interaction volume (1 mm spot size × 0.1 mm path length). The magnitude of the *T*-jump was calibrated using the D<sub>2</sub>O absorbance change at the corresponding probing frequency.<sup>12</sup> A CW lead salts infrared diode laser (Laser Analytics) serves as the probe, which is tunable from 1550 to 1800 cm<sup>-1</sup>. Transient absorbance changes of the probe induced by the *T*-jump pulses were detected by a 50 MHz MCT detector (Kolmar Technologies). Digitization of the signal was accomplished by a Tektronix TDS 3052 digital oscilloscope. As in the static FTIR measurements, a sample cell with dual compartments and a 100 μm path length was used to allow the separate measurements of the sample and reference (D<sub>2</sub>O) under identical conditions. The D<sub>2</sub>O measurements provide the information for both *T*-jump calibration<sup>4</sup> and background subtraction. The D<sub>2</sub>O IR absorption spectrum is temperature dependent near the amide I' absorption band region, thus quantitative subtraction of the reference spectrum at each temperature is essential.

## Results and Discussion

The α-helical peptide used in this study was based on a derivative of a poly-Ala helix originally described by Marqusee and Baldwin<sup>13</sup> with a capping group, D-Arg, incorporated at the C-terminus. We have demonstrated that the D-Arg carboxamide auxiliary is an efficient C-capping residue with  $\Delta\Delta G_C^0 = -1.2 \text{ kcal/mol}$ .<sup>14</sup> The peptide has the following sequence: Ac-YGG(KAAAA)<sub>3</sub>-CO-D-Arg-CONH<sub>2</sub> (the D-Arg peptide).

Far-UV CD spectra (data not shown) of the D-Arg peptide at low temperatures show typical features associated with α-helices. As observed for other small peptides,<sup>4–7</sup> the thermal unfolding of the D-Arg peptide measured by the CD signal at 222 nm extends over a broad temperature range and was modeled by an apparent two-state helix–coil transition to allow comparison of our results with those of others who applied this approximation (Figure 1). Specifically, the mean residue ellipticities at 222 nm,  $\theta_{222}$ , which are linearly related to mean helix content, were fitted by the following equation

$$\theta_{222} = (\theta_H - \theta_C)/(1 + K_{eq}) + \theta_C \quad (1)$$

where  $K_{eq}$  is the equilibrium constant for unfolding and  $\theta_H$  and  $\theta_C$  are the baseline ellipticities of both the helix and the random coil. In the fitting, the values of  $\theta_H$  and  $\theta_C$  were evaluated using the following expressions given by Luo and Baldwin<sup>15</sup>

(13) Marqusee S.; Baldwin R. L. *Proc. Natl. Acad. Sci. U.S.A.* **1987**, *84*, 8898–8902.

(14) Schneider, J. P.; DeGrado, W. F. *J. Am. Chem. Soc.* **1998**, *120*, 2764–2767.

(15) Rohl, C. A.; Baldwin, R. L. *Biochemistry* **1997**, *36*, 8435–8442.

(16) Becketl, W. J.; Schellman, J. A. *Biopolymers* **1987**, *26*, 1859–1977.

(17) If both  $\theta_H$  and  $\theta_C$  were assumed to be temperature independent and treated as fitting parameters, the following thermodynamic parameters were obtained from the fit:  $\theta_H = -30345 \text{ deg cm}^2 \text{ dmol}^{-1}$ ,  $\theta_C = -2514 \text{ deg cm}^2 \text{ dmol}^{-1}$ ,  $T_m = 8.9 \text{ °C}$ ,  $\Delta H = 11.7 \text{ kcal/mol}$ ,  $\Delta S = 41.7 \text{ cal/(mol K)}$ , and  $\Delta C_p = 0$ .

(18) Krimm S.; Bandekar, J. *Adv. Protein Chem.* **1986**, *38*, 181–364. Heimburg, T.; Schuenemann, J.; Weber, K.; Geisler, N. *Biochemistry* **1996**, *35*, 1375–1382. Gilmanshin, R.; Williams, S.; Callender, R. H.; Woodruff, W. H.; Dyer, R. B. *Biochemistry* **1997**, *36*, 15006–15012. Volk, M.; Kholodenko, Y.; Lu, H. S. M.; Gooding, E. A.; DeGrado, W. F.; Hochstrasser, R. M. *J. Phys. Chem. B* **1997**, *101*, 8607–8616. Dyer, R. B.; Gai, F.; Woodruff, W. H.; Gilmanshin, R.; Callender, R. H. *Acc. Chem. Res.* **1998**, *31*, 709–716.

(19) Nesmelova, I.; Krushelnitsky, A.; Idiyatullin, D.; Blanco, F.; Ramirez-Alvarado, M.; Daragan, V. A.; Serrano, L.; Mayo, K. H. *Biochemistry*, **2001**, *40*, 2844–2853.

(20) Schwarz, G. *J. Mol. Biol.* **1965**, *11*, 64–77.

(21) Shimada, J.; Kussell, E. L.; Shakhnovich, E. I. *J. Mol. Biol.* **2001**, *308*, 79–95.

(22) Vila, J. A.; Ripoll, D. R.; Scheraga, H. A. *Proc. Natl. Acad. Sci. U.S.A.* **2000**, *97*, 13075–13079. Vila, J. A.; Ripoll, D. R.; Scheraga, H. A. *Biopolymers* **2001**, *58*, 235–246.

(23) For a two-state relaxation process,  $k_{\text{obs}} = k_f + k_u$ ,  $K_{eq} = k_f/k_u$ .

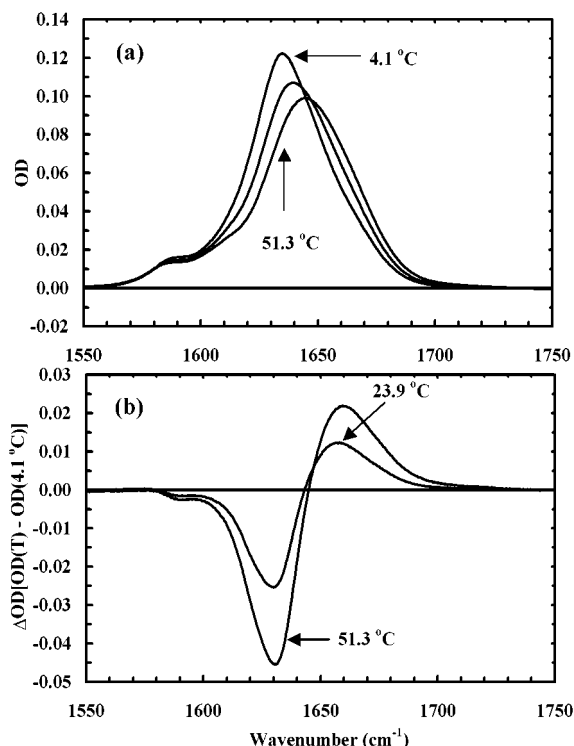


**Figure 2.** (a) Equilibrium FTIR spectra of the D-Arg peptide in D<sub>2</sub>O solution measured at 4.1, 23.9, and 51.3 °C, respectively. The equilibrium FTIR spectra of the D-Arg peptide were found to be fully reversible as a function of temperature, indicating that no peptide aggregation occurs at the concentration used and to the highest temperature, 70 °C. (b) Difference FTIR spectra generated by subtracting the spectrum collected at 4.1 °C from the spectra collected at 23.9 and 51.3 °C, respectively.

$$\theta_C = 2220 - 53T \quad (2a)$$

$$\theta_H = (-44000 + 250T)(1 - 3/N_R) \quad (2b)$$

where  $T$  is the temperature in Celsius and  $N_R$  is the helical chain length in residues. The temperature-dependent equilibrium constant,  $K_{eq}$ , was calculated using following equations<sup>16</sup>

$$K_{eq} = \exp(-\Delta G/RT) \quad (3)$$

$$\Delta G = \Delta H + \Delta C_p(T - T_m) - T[\Delta S + \Delta C_p \ln(T/T_m)] \quad (4)$$

where  $T_m$  is the thermal melting temperature and  $\Delta H$ ,  $\Delta S$ , and  $\Delta C_p$  are the enthalpy, entropy, and heat capacity changes, respectively. The best fit (Figure 1) yields the following thermodynamic parameters:<sup>17</sup>  $T_m = 10$  °C,  $\Delta H = 7.8$  kcal/mol,  $\Delta S = 27.5$  cal/(mol K), and  $\Delta C_p = 0$ .

Compared to the Fs peptide, the D-Arg peptide is less stable, presumably due to the shorter helix forming segment as well as Lys residue at the N-terminus whose positive charge interacts unfavorably with the helix dipole moment.

Temperature-dependent infrared spectra in the amide I' region (Figure 2a) show that the solvated helix in D<sub>2</sub>O has an amide I' absorbance centered at  $\sim 1636$  cm<sup>-1</sup>. The amide I' IR absorbance is due mainly to the C=O stretch vibration. Its sensitivity to conformation renders it a good structural reporter.<sup>18</sup> As indicated by the FTIR difference spectra (Figure 2b), the amide I' band loses intensity as temperature increases, with the concurrent formation of a new spectral feature at higher energy. The negative feature, centered around 1632 cm<sup>-1</sup>, is due to the loss of helical structures, and the positive feature, centered at

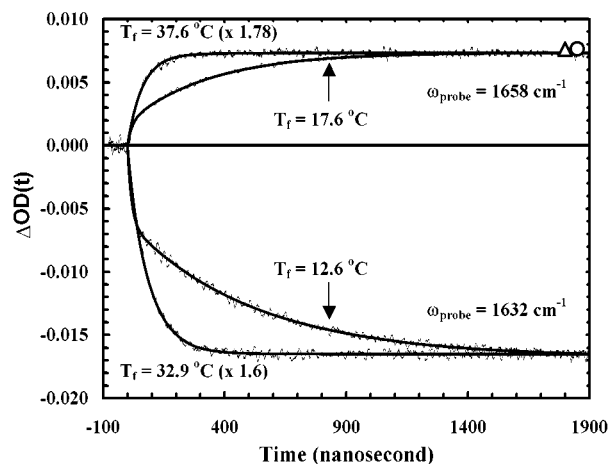


**Figure 3.** Representative relaxation traces corresponding to different final temperatures and probing frequencies. The amplitude of the  $T$ -jump was  $\sim 10$  °C for each case. The data collected at higher temperatures were scaled, as indicated in the plot, to reflect the difference between two relaxations obtained at the same frequency but different final temperatures. The solid lines are fits to the following function,  $OD(t) = A[1 - B \exp(-t/\tau)]$ , convolved with the instrument response function that was determined by the response of the detection system to the 3 ns pump pulse. Here  $A$  is the full amplitude of the signal and  $B$  is the relative amplitude of the slow phase, which has a lifetime  $\tau$ . For all the data measured, the relative amplitude of the slow phase varies between 62 and 78%, without systematic trend. For the data presented here, the relative amplitudes of the slow phase are as follows:  $B(32.9$  °C) = 76%,  $B(12.6$  °C) = 62%,  $B(37.6$  °C) = 69%, and  $B(17.6$  °C) = 71%.  $\circ$  and  $\triangle$  are the equilibrium amplitudes obtained from the equilibrium FTIR spectra corresponding to the same initial and final temperatures as those used for the two kinetic traces probed at 1658 cm<sup>-1</sup>. Note that the equilibrium amplitudes have been scaled to reflect the sample conditions (path length and concentration) as well as the scaling factor used for the kinetics data.

$\sim 1665$  cm<sup>-1</sup>, corresponds to the formation of random coil conformations. The relaxation kinetics following a  $T$ -jump, due to the loss of the helical structure or the formation of the random coil, can be studied by probing the corresponding spectral features.

The relaxation kinetics following a  $T$ -jump (Figure 3) show two well-resolved phases that can be described by a biexponential function. These results are consistent with Thompson and co-worker's simulations<sup>5</sup> based on a "kinetic zipper" model for the helix-coil transition. This model suggests that the fast phase is associated with the redistribution of the helix lengths and proceeds in several nanoseconds, in agreement with our results (Figure 3). The fast component rises instantaneously and is therefore estimated to be faster than 20 ns (the response time of the infrared detector), and the slow component has a lifetime of 140 ns at 27 °C, in good agreement with the 160 ns obtained by Williams et al.<sup>4</sup> When temperature decreases to 4 °C, the slow relaxation time increases to ca. 1.4  $\mu$ s, which agrees well with the 4  $\mu$ s exchange lifetime of a helix-forming peptide at 5 °C observed by Nesselova et al.<sup>19</sup> in a <sup>13</sup>C NMR relaxation experiment. They attribute this exchange mainly to the helical peptide folding-unfolding.

In contrast to the Schwarz model,<sup>20</sup> the slow component has a fairly large and monotonic temperature dependence (Figure 4). This model essentially suggests a chevron-type temperature dependence for the slow relaxation rate that exhibits a minimum near the thermal melting temperature. Since the lowest temperature measured in this study is ca. 4 °C, whereas the thermal melting temperature of the D-Arg peptide is 10 °C, it is unlikely that we have only observed the linear part of a chevron curve.

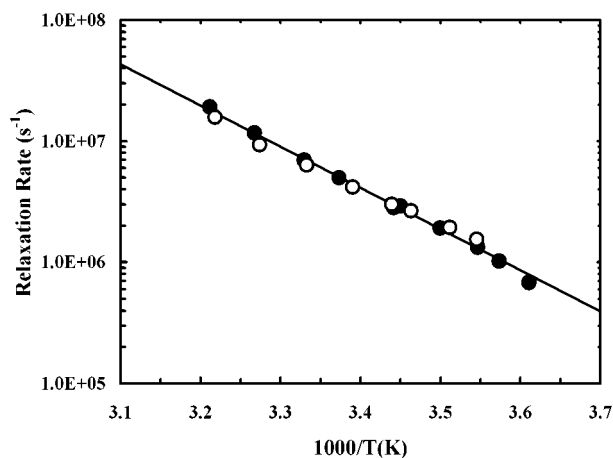


**Figure 4.** Arrhenius plot of the slow relaxation rates measured at 1632 (filled circles) and 1658  $\text{cm}^{-1}$  (open circles). Linear regression to these data (solid line) yields an apparent activation energy of 15.5 kcal/mol.

Although the current result is consistent with other studies,<sup>6,7,19</sup> the observed apparent activation energy for the slow phase is roughly twice the value measured for other peptides. Such a big difference is unlikely due to the result of uncertainties in different experiments. One possible explanation is that this difference is simply representative of the difference between peptides used. For example, in a recent all-atom Monte Carlo simulation, Shimada et al.<sup>21</sup> suggested that the slow phase observed for the Fs peptide is due to the slow incorporation of the Arg residue, which has a greater entropic penalty, into the growing helix. Differences in the number and position of Lys residues might similarly affect the stability and kinetics of helix formation of the D-Arg peptide. Recent studies by Scheraga and co-workers<sup>22</sup> have also shown that residues with long polar or charged side chains, such as Lys, have a large effect on the stability of helix conformations.

The refolding rate constants corresponding to the slow phase may be calculated by using the equilibrium constants obtained from CD measurements as well as a two-state model.<sup>23</sup> Such an analysis yields an activation energy of 11.3 kcal/mol for helix formation, in contrast to the  $-1$  kcal/mol refolding activation energy reported by Lednev et al.<sup>7</sup> However, one should note that this type of analysis is only valid for real two-state processes, whereas the thermal unfolding of helical peptides is multi-state, not two-state, as suggested by this work and other studies.<sup>26</sup>

More studies need to be carried out to identify the origin of the fast relaxation process and its temperature dependence. If this fast phase corresponds to the  $\sim 20$  ns relaxation process observed by Thompson et al. through an N-terminal fluorescent probe in the Fs peptide,<sup>5</sup> we should be able to resolve this component directly with a faster infrared detector.<sup>24</sup> As suggested by Thompson et al., the slow relaxation process may involve the initial nucleation steps. If so, the fairly large activation energy for this process suggests that the energy barrier for the coil to helix transition is not purely entropic and the solvent may play an important role in controlling the helix–

coil transition rates.<sup>6</sup> For example, Kramers' theory suggests that in the high friction limit the reaction rate is inversely proportional to the solvent viscosity. The reciprocal dependence of the rate constant on the solvent viscosity would produce an additional apparent activation energy of approximately 4.5 kcal/mol,<sup>25</sup> due to the temperature dependence of the solvent ( $\text{D}_2\text{O}$ ) viscosity.

A recent stopped-flow CD study of helix–coil transition by Clarke et al.<sup>26</sup> suggests that the nucleation process may be much slower than previously thought, on the millisecond time scale. Using a 16-residue peptide (the AK16 peptide), Ac-YGA-AKAAAAKAAA-AKA-NH<sub>2</sub>, they observed a folding rate constant of 15  $\text{s}^{-1}$  at 0 °C. Clearly, this rate is considerably slower than that measured in this work or by the <sup>13</sup>C NMR relaxation method.<sup>19</sup> Although the longest time probed in our study is only ca. 2  $\mu\text{s}$ , the good agreement between the relaxation amplitude and the equilibrium amplitude (Figure 3) indicates that there are no kinetic events present on longer time scales.

Clearly, the multiexponential relaxation kinetics show that the helix–coil transition is not a two-state process. Deviations from single-exponential kinetics could be due to reaction intermediates or multiple reaction pathways or both. With a conformation probe that reports only on average helix content, such as IR, it is difficult to distinguish these possibilities. A site-specific conformation probe, such as <sup>13</sup>C labeled amino acids (see below), should provide better insights into the understanding of the helix–coil transition. The amide I absorbance is sensitive to isotopic substitution.<sup>27</sup> Peptides with <sup>13</sup>C labeled amino acids at strategically important positions would provide unique model systems to study the helix–coil transition.<sup>27</sup> When coupled with the T-jump method, this isotope-editing technique can potentially reveal detailed information at the single residue level regarding the nucleation and propagation steps along the helix folding pathways. Such studies are currently underway.

It is worth noting that a recent all-atom computer simulation carried out by Elmer and Pande<sup>28</sup> as well as an experimental study done by Yang et al.<sup>29</sup> on nonbiological helices show that the nonbiological helix–coil transition also exhibits nonexponential relaxation kinetics, in agreement with what we observed in this study and also demonstrating the complex nature of folding even for simple synthetic structure-forming oligomers.

## Conclusion

We have studied the temperature dependence of the helix–coil transition of the D-Arg peptide, Ac-YGG(KAAAA)<sub>3</sub>-CO-D-Arg-CONH<sub>2</sub>. Its relaxation kinetics following a T-jump are nonexponential, indicating that the helix–coil transition is not a two-state process. The slow component, which has a relaxation time constant ca. 140 ns at 300 K, exhibits a linear temperature dependence that gives rise to an apparent activation energy of 15.5 kcal/mol.

**Acknowledgment.** F.G. gratefully acknowledges financial support from Research Corporation, the University of Pennsylvania Research Foundation, and the NSF (CHE-0094077). J.W.K. was supported by NIH grant AG10599.

JA0158814

(24) With improved time resolution, we have recently observed a similar fast relaxation component,  $\sim 20$  ns, in the relaxation kinetics of the Fs peptide following a T-jump.

(25) Cho, C. H.; Urquidi, J.; Singh, S.; Robinson, G. W. *J. Phys. Chem. B* **1999**, *103*, 1991–1994.

(26) Clarke, D. T.; Doig, A. J.; Stapley, B. J.; Jones, G. R. *Proc. Natl. Acad. Sci. U.S.A.* **1999**, *96*, 7232–7237.

(27) Decatur S. M.; Antonic J. *J. Am. Chem. Soc.* **1999**, *121*, 11914–11915. Decatur S. M. *Biopolymers* **2000**, *54*, 180–185. Silva, R. A. G. D.; Kubelka, J.; Bour, P.; Decatur, S. M.; Keiderling, T. A. *Proc. Natl. Acad. Sci. U.S.A.* **2000**, *97*, 8318–8323.

(28) Elmer, S.; Pande V. S. *J. Phys. Chem. B* **2001**, *105*, 482–485.

(29) Yang, W. Y.; Prince, R. B.; Sabelko, J.; Moore, J. S.; Gruebele, M. *J. Am. Chem. Soc.* **2000**, *122*, 3248–3240.